The Journal of Immunology

RESEARCH ARTICLE | MAY 01 2002

TNF Regulates Chemokine Induction Essential for Cell Recruitment, Granuloma Formation, and Clearance of Mycobacterial Infection[1] FREE

Daniel R. Roach; ... et. al

J Immunol (2002) 168 (9): 4620–4627.
https://doi.org/10.4049/jimmunol.168.9.4620

TNF Regulates Chemokine Induction Essential for Cell Recruitment, Granuloma Formation, and Clearance of Mycobacterial Infection[1]

Daniel R. Roach,* Andrew G. D. Bean,[2]* Caroline Demangel,*‡ Malcolm P. France,§ Helen Briscoe,*† and Warwick J. Britton[3]*†

Host immunity to mycobacterial infection is dependent on the activation of T lymphocytes and their recruitment with monocytes to form granulomas. These discrete foci of activated macrophages and lymphocytes provide a microenvironment for containing the infection. The cytokine, TNF, is essential for the formation and maintenance of granulomas, but the mechanisms by which TNF regulates these processes are unclear. We have compared the responses of TNF-deficient ($TNF^{-/-}$) and wild-type C57BL/6 mice to infection with *Mycobacterium smegmatis*, a potent inducer of TNF, and virulent *Mycobacterium tuberculosis* to delineate the TNF-dependent and -independent components of the process. The initial clearance of *M. smegmatis* was TNF independent, but TNF was required for the early expression of mRNA encoding C-C and C-X-C chemokines and the initial recruitment of $CD11b^+$ macrophages and $CD4^+$ T cells to the liver during the second week of infection. Late chemokine expression and cell recruitment developed in $TNF^{-/-}$ mice associated with enhanced Th1-like T cell responses and mycobacterial clearance, but recruited leukocytes did not form tight granulomas. Infection of $TNF^{-/-}$ mice with *M. tuberculosis* also resulted in an initial delay in chemokine induction and cellular recruitment to the liver. Subsequently, increased mRNA expression was evident in $TNF^{-/-}$ mice, but the loosely associated lymphocytes and macrophages failed to form granulomas and prevent progressive infection. Therefore, TNF orchestrates early induction of chemokines and initial leukocyte recruitment, but has an additional role in the aggregation of leukocytes into functional granulomas capable of controlling virulent mycobacterial infection. *The Journal of Immunology,* **2002, 168: 4620–4627.**

The formation of granulomas at the site of mycobacterial infection is an essential component of host immunity for controlling infection. This process is dependent on the activation of mycobacteria-reactive T lymphocytes (1), particularly IFN-γ-secreting $CD4^+$ and $CD8^+$ T cells (2, 3). Granuloma formation, however, is a complex process that requires not only the activation of the lymphocytes, but also their recruitment with monocytes to the site of the infection, migration into the tissues, and juxtaposition around mycobacteria-infected macrophages (4). This colocation facilitates the activation of bactericidal mechanisms in infected macrophages by T cell-derived cytokines (1). Some mycobacteria, however, survive within macrophages, and persistent antigenic stimulation perpetuates the process leading to chronic granuloma formation characterized by dense accumulations of infected macrophages, epithelioid cells, and T lymphocytes (5). These granulomas contain the mycobacterial infection and prevent dissemination to other organs, but they are also responsible for lung immunopathology, as the granulomas displace and destroy parenchymal tissue (6). The cytokine and chemokine signals that regulate granuloma formation and persistence are poorly understood, although signaling through TNF receptor I plays an essential role (7, 8).

TNF (previously known as TNF-α) is a highly potent proinflammatory cytokine with a wide range of activities in both inflammatory and immune responses (9). TNF (8, 10) and the related cytokine lymphotoxin-α (LTα)[4] (11) are essential for host resistance against infection with *Mycobacterium tuberculosis* and other mycobacteria. TNF-deficient ($TNF^{-/-}$) mice infected by aerosol with *M. tuberculosis* develop normal T cell responses to mycobacterial Ags (10), but are profoundly susceptible to the infection, succumbing with extensive necrosis in the lungs and infected organs. A major defect is the failure of granuloma formation in the infected organs of $TNF^{-/-}$ mice. Dissecting the effects of TNF deficiency on the sequential steps involved in granuloma formation in the lung is hampered in *M. tuberculosis* infection by the rapidly progressive necrosis associated with an influx of neutrophils observed in these mice. By comparison, infection with less virulent mycobacteria allows analysis of the effects of TNF deficiency on the induction of chemokines and recruitment of leukocytes into granulomas.

Mycobacterium smegmatis is a rapidly growing mycobacterium that is usually nonpathogenic in immunocompetent subjects. A

∗Centenary Institute of Cancer Medicine and Cell Biology, Sydney, Australia; †Department of Medicine, University of Sydney, Sydney, Australia; ‡Laboratoire d'Ingenierie des Anticorps, Institut Pasteur, Paris, France; and §Department of Veterinary Anatomy and Pathology, University of Sydney, Sydney, Australia

Received for publication December 17, 2001. Accepted for publication February 28, 2002.

The costs of publication of this article were defrayed in part by the payment of page charges. This article must therefore be hereby marked *advertisement* in accordance with 18 U.S.C. Section 1734 solely to indicate this fact.

[1] This work was supported by the National Health and Medical Research Council of Australia, New South Wales Health Department Research and Infrastructure Grant program, and a University of Sydney Postgraduate Award (to D.R.R.).

[2] Current address: CSIRO Livestock Industries, Geelong, Victoria 3220, Australia.

[3] Address correspondence and reprint requests to Prof. Warwick J. Britton, Centenary Institute of Cancer Medicine and Cell Biology, Locked Bag 6, Newtown, 2042 New South Wales, Australia. E-mail address: wbritton@medicine.usyd.edu.au

[4] Abbreviations used in this paper: LTα, lymphotoxin-α; BCG, bacille Calmette-Guérin; araLAM, arabinan side chains of lipoarabinomannan; iNOS, inducible NO synthase; LAM, lipoarabinomannan; manLAM, mannan caps of lipoarabinomannan; MIP-1α, macrophage-inflammatory protein-α; MCP-1, macrophage chemoattractive protein-1; RNI, reactive nitrogen intermediate; WT, wild type.

0022-1767/02/$02.00

major component of mycobacterial cell wall is lipoarabinomannan (LAM), which is a complex polysaccharide composed of arabinan and mannan linked to the cell membrane by phosphatidylinositol (12). In the case of *M. smegmatis* and the avirulent H37Ra strain of *M. tuberculosis*, LAM is characterized by extensive arabinan side chains (araLAM), whereas in LAM from more virulent mycobacteria (*M. tuberculosis* H37RV and *Mycobacterium bovis)* the arabinan side chains are masked by mannan caps (manLAM) (13, 14). These forms of LAM differ markedly in their ability to stimulate TNF production from human and mouse macrophages (15, 16), with purified araLAM inducing more TNF secretion than purified manLAM. Therefore, it was proposed that mycobacterial virulence may be related in part to this differential induction of TNF by the two forms of LAM, with avirulent mycobacteria stimulating increased TNF production resulting in enhanced macrophage bactericidal activities and early clearance of the organisms (15). In this report, we have compared infection with *M. smegmatis* and *M. tuberculosis* infection in TNF-deficient ($TNF^{-/-}$) and normal mice (wild type (WT)). We found that the initial clearance of *M. smegmatis* during the first week of infection was independent of TNF, but subsequently TNF deficiency resulted in delayed expression of chemokines and reduced cellular recruitment associated with delayed clearance of *M. smegmatis*. The emergence of an enhanced Th1-like T cell response was associated with the late induction of chemokines and control of the infection. By comparison, infection of $TNF^{-/-}$ mice with virulent *M. tuberculosis* was associated with an initial delay in chemokine induction and cellular infiltrate into the liver. Then, despite excessive chemokine production, there was a failure to form functional granulomas, resulting in fatal progressive infection. Therefore, although TNF is not essential for chemokine expression per se, it is required both for the early induction of chemokines that initiates timely cell recruitment and for establishing and maintaining the microenvironment of protective granulomas.

Materials and Methods

Mice

Control WT mice were 6- to 8 wk-old C57BL/6 mice obtained from the Animal Resource Center (Perth, Australia). TNF gene knockout mice ($TNF^{-/-}$) prepared on a C57BL/6 background have been previously described (17). All mice were housed under specific pathogen-free conditions in the Centenary Institute animal facility until infection, when they were transferred and maintained in a level 2 (*M. smegmatis*) or level 3 (*M. tuberculosis*) physical containment facility.

Bacteria and experimental infections

M. smegmatis (mc^2155) was grown in Middlebrook 7H9 liquid medium (Difco, Detroit, MI) supplemented with ADC for 7 days at 37°C. *Mycobacterium bovis* (bacille Calmette-Guérin (BCG)) was derived from the Glaxo strain; it was obtained from CSL Biosciences (Melbourne, Australia) and was cultured as described for *M. smegmatis*. The *M. tuberculosis* $H_{37}Rv$ (ATCC 27294; American Type Culture Collection, Manassas, VA) strain was cultured from a low passage seed lot in Proskauer-Beck liquid medium to midlog phase, aliquoted, and frozen at −70°C. $TNF^{-/-}$ and WT mice were infected with 5×10^7 CFU *M. smegmatis* or 1×10^4 CFU *M. tuberculosis* via a lateral tail vein. The numbers of viable bacteria in target organs were followed over time by plating serial dilutions of whole organ homogenates on supplemented Middlebrook 7H11 agar (Difco) and counting bacterial colony formation after 3 days (*M. smegmatis*) or 21 days (*M. tuberculosis*) of culture. *M. smegmatis* sonicate was prepared by sonication in PBS as previously described (18) and was stored at −70°C.

Macrophage infections

Bone marrow-derived macrophages were cultured from murine bone marrow as previously described (11). After 7 days of culture, these cells were either prestimulated with 100 U/ml IFN-γ (Genzyme, Cambridge, MA) or medium alone for 18 h and then infected with *M. smegmatis* or *M. bovis* (BCG) at a multiplicity of infection of 10:1 for 6 h. Cells were washed to remove extracellular bacteria and were cultured for 4 days. The concentration of TNF in the culture supernatants was measured using the WEHI 164 bioassay, as previously described (11).

Liver leukocyte preparations

Animals were sacrificed by carbon dioxide narcosis, and the liver was perfused with saline through the portal vein to remove blood-borne leukocytes. A single-cell suspension was prepared by sieving a liver lobe through a 200-μm pore size mesh. Liver leukocytes were obtained by spinning the suspension over an isotonic Percoll gradient (Pharmacia Biotech, Uppsala, Sweden). The number of leukocytes in each preparation was counted using a Sysmex KX-21 hemocytometer (TOA Medical Electronics, Kobe, Japan). Flow cytometric analysis of each cell preparation was performed as previously described (3) to determine the number of $CD11b^+$ (M1/70.15; Caltag Laboratories, San Francisco, CA) and $CD4^+$ (CT-CD4; Caltag Laboratories) T cells in the sample.

Analysis of chemokine mRNA

Expression of chemokine mRNA in the livers of infected mice was measured using the RiboQuant RNase protection assay system (BD PharMingen, San Diego, CA) according to the manufacturer's instructions. Briefly, a ^{32}P-labeled multiprobe template set specific for lymphotactin, RANTES, eotaxin, macrophage-inflammatory protein-α (MIP-1α), MIP-1β, MIP-2, monocyte chemoattractant protein-1 (MCP-1), and T cell activation-3 and 2 constitutively expressed genes GADPH and L32 was generated. Total liver RNA from uninfected and *M. smegmatis*-infected or *M. tuberculosis*-infected WT and $TNF^{-/-}$ mice was prepared using RNAzol B (Cinna/Tel-Test, Friendswood, TX) according to the manufacturer's instructions, with an additional phenol-chloroform extraction before RNA precipitation. Samples of total RNA from the liver (50 μg) of uninfected and infected mice were incubated with 1.6×10^6 cpm of probe and incubated overnight at 56°C. Single-stranded RNA was digested with RNase, and the protected probes were analyzed by PAGE. Gels were dried and exposed to x-ray film or GEL-DOC 1000 detection screens (Bio-Rad, Hercules, CA). The migration distance of bands of known sizes on each gel allowed identification of the band representing each chemokine. The intensity of each band on the phosphorimager was calculated using Molecular Analyst software (Bio-Rad). Differences in the amounts of RNA between samples were corrected for by expressing band intensity as a ratio of the gene of interest to the constitutively expressed gene, L32.

T cell responses to mycobacterial Ags

Spleens from *M. smegmatis*-infected $TNF^{-/-}$ and WT mice were removed, and single-cell suspensions were prepared. Erythrocytes were lysed in a hypotonic ammonium chloride lysis buffer, and the remaining cells were washed, counted, and suspended in complete RPMI 1640 medium (Cytosystem, Sydney, Australia) with 10% FCS (Trace, Sydney, Australia), 2 mM L-glutamine (Sigma-Aldrich, St. Louis, MO), 10 mM HEPES (Sigma-Aldrich), 10 mM Na_2CO_3, 0.5 μM 2-ME (Sigma-Aldrich), 100 U/ml penicillin (Trace), and 100 μg/ml streptomycin (CSL). To measure Ag-specific T cell responses, splenocytes from *M. smegmatis*-infected cells were cultured in the presence of *M. smegmatis* sonicate (10 μg/ml) or in medium alone. Lymphocyte proliferation and cytokine assays for IFN-γ were performed as described previously (19). For proliferative responses, the cells were pulsed with 1 μCi of [^{3}H]thymidine (NEN Life Sciences, Boston, MA) for the final 6 h of culture and then harvested onto glass fiber filters. The incorporated [^{3}H]thymidine was determined by liquid scintillation spectroscopy (Pharmacia/Wallace Oy, Turku, Finland). Specific [^{3}H]thymidine incorporation was calculated by subtracting the mean counts per minute in unstimulated wells from the mean counts per minute of test samples. The concentration of IFN-γ in culture supernatants was determined with a capture ELISA using a mAb capture assay with the Abs R4-6A2 and XMG1.2-biotin (Endogen, Woburn, MA) following the manufacturer's instructions. Avidin-alkaline phosphatase (Sigma-Aldrich) and *n*-nitro-phenyl-phosphate (1 mg/ml in 10 mM $NaHCO_3$ and 0.1 mM $MgCO_3$, pH 6.3) were used as the colorimetric reagents, and absorbance was measured at 405 nm. Proliferation and IFN-γ release from uninfected WT and $TNF^{-/-}$ mice were insignificant. To determine the frequency of IFN-γ-producing cells, splenocytes were cultured in multiscreen 96-well filtration plates (Millipore, Bedford, MA) for 16 h in the presence of *M. smegmatis* sonicate or medium alone. The ELISPOTs were then developed as previously described (19).

Histology

Liver tissue samples were fixed in 10% neutral buffered Formalin, processed into paraffin blocks, and sectioned at 5 μm. Sections were stained with H&E, coded, and analyzed in a blinded fashion to assess the number

and type of infiltrating leukocytes in the livers of WT and TNF$^{-/-}$ mice. A focus of inflammatory cells (foci) was defined as a collection of 10 or more macrophages and lymphocytes in a cluster.

Serum nitrite measurements

Serum nitrite was assayed by a modification of the nitrate kit for food analysis (Roche, Mannheim, Germany). Briefly, serum nitrate was reduced to nitrite using nitrate reductase. Nitrite levels in the samples were determined using the Greiss reagent (3% phosphoric acid, 1% *p*-amino-benzenesulfonamide, and 1% *n*-1-napthylenediamide (Sigma-Aldrich)). Samples were incubated for 5 min at room temperature, and absorbance was measured at 540 nm.

Statistical analysis

Where appropriate, values were tested for statistical significance by unpaired Student's *t* test using StatView (SAS Institute, Cary, NC). Colony-forming unit values were subjected to $\log_{10}$ transformation before analysis.

Results

M. smegmatis *infection elicits increased TNF production from macrophages compared with* M. bovis *(BCG) infection*

To test whether *M. smegmatis* as an avirulent mycobacteria was more potent in inducing TNF than a more virulent species, bone marrow-derived macrophages were infected with either *M. smegmatis* or *M. bovis* (BCG), and the production of TNF was monitored over time. Macrophages infected with *M. smegmatis* produced significantly larger amounts of TNF than those infected with *M. bovis* BCG over 72 h of culture (Fig. 1*A*; $p < 0.05$). Prestimulation of the macrophages for 16 h with IFN-γ (100 U/ml) abrogated this difference, such that macrophages infected with either *M. smegmatis* or *M. bovis* (BCG) produced comparable amounts of TNF (Fig. 1*B*).

Clearance of bacteria is delayed in TNF$^{-/-}$ mice infected with M. smegmatis

TNF$^{-/-}$ and WT mice were infected with *M. smegmatis*, and the clearance of bacteria from the primary sites of infection, the liver and spleen, was monitored over time. Both WT and TNF$^{-/-}$ mice controlled the infection in the liver (Fig. 2*A*) and spleen (Fig. 2*B*) to an equivalent extent over the first 7 days following infection. The rapid clearance of bacteria continued over the following 14 days in WT mice. In contrast, bacterial clearance significantly slowed after 7 days in TNF$^{-/-}$ mice. There were significantly more bacteria in the liver and spleen of TNF$^{-/-}$ mice at 14 and 21 days postinfection compared with WT mice ($p < 0.05$). After day 21 the clearance rate in TNF$^{-/-}$ increased, so that by 28 days postinfection bacteria were cleared from both WT and TNF$^{-/-}$ mice.

Cell recruitment is delayed in TNF$^{-/-}$ mice infected with M. smegmatis

To determine whether the delay in clearance of bacteria was associated with differences in the recruitment of leukocytes to the sites of infection and subsequent granuloma formation, the histological appearance and cellular infiltrate in the liver were examined over the course of infection in both WT and TNF$^{-/-}$ mice. In WT mice, a florid monocytic infiltrate was generated. The number of foci of inflammatory cells (Fig. 3*A* and Fig. 4, *A* and *C*) and the total number of leukocytes recruited into the liver (Fig. 3*B*) peaked on day 14 postinfection in WT mice and then declined by day 28 postinfection. By contrast, recruitment of leukocytes into the liver and subsequent formation of foci of inflammatory cells were significantly delayed in TNF$^{-/-}$ mice following infection with *M. smegmatis* (Fig. 3, *A* and *B*, and Fig. 4, *B* and *D*). In the absence of TNF, liver leukocyte numbers did not increase until day 21 postinfection, and by day 28 the cellular infiltrate of lymphocytes and macrophages was still only loosely clustered. Flow cytometric analysis of the isolated liver leukocytes from the WT mice demonstrated that the influx of macrophages (CD11b$^+$; Fig. 3*C*) and CD4$^+$ T cells (Fig. 3*D*) peaked on days 7 and 14, respectively. In the TNF$^{-/-}$ mice, the recruitment of CD11b$^+$ cells and CD4$^+$ T cells was markedly delayed (Fig. 3, *C* and *D*), although the absolute rise in numbers of CD4$^+$ T cells was greater in TNF$^{-/-}$ than in WT controls.

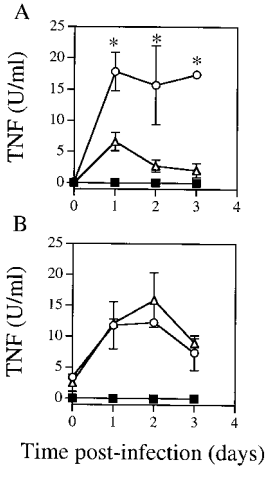

FIGURE 1. TNF production from bone marrow-derived macrophages following infection with different mycobacterial species. Bone marrow-derived macrophages were infected with either *M. smegmatis* (MOI 10:1; ○) or *M. bovis* (BCG; multiplicity of infection, 10:1; △) or were uninfected (■). TNF production was measured by the WEHI 164 bioassay. *A*, No prestimulation; *B*, prestimulated with 100 U/ml IFN-γ for 16 h. The data are the mean ± SEM of triplicate wells and are representative of one of two experiments. Significant differences between TNF production in *M. smegmatis*- and *M. bovis* (BCG)-infected cultures (*, $p < 0.05$) were determined using Student's *t* test.

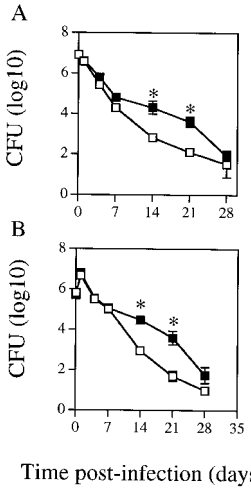

FIGURE 2. Bacterial load in WT and TNF$^{-/-}$ mice following infection with *M. smegmatis*. WT (□) and TNF$^{-/-}$ (■) mice were infected i.v. with 5×10^7 CFU of *M. smegmatis*, and the numbers of viable bacteria present in liver (*A*) and spleen (*B*) were determined over time. The data points are the mean ± SEM of the mycobacterial colony-forming units from five mice per time point and are representative of one of three similar experiments. Significant differences between TNF$^{-/-}$ and WT mice (*, $p < 0.05$) were determined by Student's *t* test and are representative of one of three experiments.

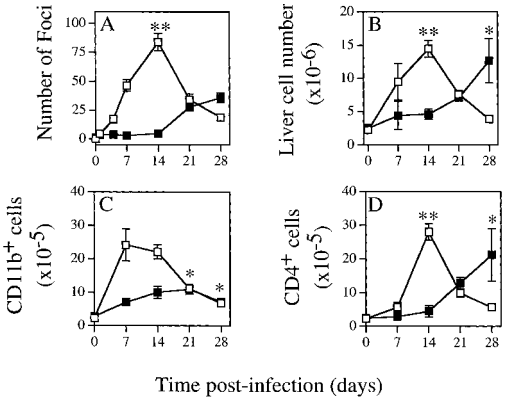

FIGURE 3. Recruitment of cells into the liver of WT (□) and TNF$^{-/-}$ (■) mice following infection with *M. smegmatis*. *A*, Number of foci of inflammatory cells in 10 high-power fields (×400). *B*, Total leukocyte number recovered from the liver. *C* and *D*, Numbers of CD11b$^+$ leukocytes (*C*) and CD4$^+$ T cells (*D*) isolated from the livers of infected mice. The data are the mean ± SEM of five mice and are representative of one of two experiments. Significant differences between WT and TNF$^{-/-}$ mice (*, $p < 0.05$; **, $p < 0.02$) were determined using Student's *t* test.

Induction of chemokines is delayed in TNF$^{-/-}$ mice

To determine the parameters of chemokine induction after *M. smegmatis* infection, the relative expression of mRNA for several chemokines in the liver was measured by RNase protection assays. Both the kinetics and pattern of chemokine induced differed between WT and TNF$^{-/-}$ mice (Fig. 5). In WT mice, increased transcription for RANTES and MCP-1 was evident on day 7 postinfection. mRNA for RANTES, MIP-1β, MIP-1α, MIP-2, MCP-1, and eotoxin were up-regulated in the liver (Fig. 5), with expression peaking on day 14 postinfection (Fig. 6). In contrast, induction of chemokine mRNA in TNF$^{-/-}$ was delayed over the first 2 wk of infection, but from day 21 chemokine expression developed independently of TNF (Fig. 5). Induction of MIP-2 mRNA was first evident in TNF$^{-/-}$ mice on day 21 postinfection (Fig. 5). By day 28 MIP-1α and MIP-1β expression was comparable to levels observed in WT mice on day 14, while relatively low levels of RANTES, MIP-2, and MCP-1 were expressed (Fig. 6)

Prolonged Ag-specific T cell responses in the absence of TNF

To determine whether the delayed up-regulation of chemokines and subsequent clearance of bacteria in TNF$^{-/-}$ mice were related to differences in the T cell responses, T cell function was analyzed in WT and TNF$^{-/-}$ mice over the course of infection. Ag-specific T cell responses were observed in both WT and TNF$^{-/-}$ mice from day 14 of infection. Comparable production of IFN-γ and proliferative responses from splenic cultures were observed on days 14 and 21 postinfection in both WT and TNF$^{-/-}$ mice (Fig. 7). The responses in WT mice then declined, but continued to increase in TNF$^{-/-}$ mice, so that by day 28 postinfection a significantly enhanced T cell response was evident in TNF$^{-/-}$ mice ($p < 0.05$). This was confirmed by the observation that the frequency of Ag-specific IFN-γ-producing cells was significantly higher in TNF$^{-/-}$ mice on day 28 postinfection ($p < 0.05$; Fig. 7*C*).

Production of reactive nitrogen intermediates (RNI) is delayed in TNF$^{-/-}$ mice following infection with M. smegmatis

To monitor the production of RNI, the major bactericidal effector species for mycobacterial killing in mice, the concentration of serum nitrates were measured. In WT mice the serum nitrate concentration peaked on day 14 postinfection (Table I). In contrast, serum nitrate concentrations in TNF$^{-/-}$ mice did not peak until day 28 postinfection. The delayed production of RNI in TNF$^{-/-}$ mice was temporally associated with the increased T cell production of IFN-γ on day 28 and the final clearance of bacteria in these mice.

Cellular recruitment is delayed in TNF$^{-/-}$ mice during M. tuberculosis *infection*

To compare the regulatory actions of TNF on the induction of chemokines and the recruitment of leukocytes in response to virulent mycobacterial infection, WT and TNF$^{-/-}$ mice were infected with 1×10^4 CFU *M. tuberculosis* H37Rv i.v., and the course of infection was followed over time. As observed with aerosol *M. tuberculosis* infection, TNF$^{-/-}$ (10) mice displayed marked susceptibility to infection and succumbed to infection after ~28 days (Fig. 8*A*), with significantly increased bacterial loads in both liver (Fig. 8*B*) and spleen (data not shown). In contrast, all WT mice survived during the first 16 wk of infection (data not shown). Leukocyte infiltrate was evident in the liver of WT mice from 7 days postinfection, and by day 14 numerous well-defined granulomas were present in WT mice (Figs. 4*E* and 8*C*). By contrast, cellular recruitment in TNF$^{-/-}$ mice was significantly delayed, with very few cellular foci in the liver on day 14 (Fig. 8*C*). By day 21 cellular foci were present in livers of TNF$^{-/-}$ mice, and by day 28 these were significantly more numerous in TNF$^{-/-}$ than in WT controls (Fig. 8*C*). These cellular foci, however, differed from those in WT mice. Although they contained macrophages and lymphocytes, they did not form tight clusters typical of WT foci (Fig. 4, *G* and *H*). Furthermore, in WT mice most granulomas on day 28 contained epithelioid macrophages with a lymphocyte cuff, whereas the granulomas in TNF$^{-/-}$ mice lacked these differentiated cells. Interestingly, the large infiltration of neutrophils present in the lungs of TNF$^{-/-}$ mice during *M. tuberculosis* infection (10) did not occur in the livers of these mice, with only occasional neutrophils present.

Induction of chemokines is delayed and then increased in TNF$^{-/-}$ mice during M. tuberculosis *infection*

In WT mice chemokine expression was evident at 7 and 14 days postinfection with induction of mRNA for RANTES, MIP-1β, MIP-2, and MCP-1 (Fig. 9). In TNF$^{-/-}$ mice the induction of these chemokines was delayed, with significantly less chemokine mRNA expression in the first 2 wk of infection. However, the expression of chemokine mRNA was detected from day 21 in TNF$^{-/-}$ mice, with significantly increased levels of mRNA for eotaxin, MIP-1β, MIP-2, and MCP-1 compared with WT infected mice (Fig. 9). The increased levels of chemokine mRNA persisted and were higher on day 28 postinfection even though the mice were succumbing to the infection at this time.

Discussion

These models of mycobacterial infection permitted us to dissect the essential role of TNF in the induction of the chemokines and the recruitment of macrophages and T cells required to clear the intracellular bacterial infections. Infection with *M. smegmatis* is not a model of *M. tuberculosis* infection per se (20). In particular, *M. smegmatis* infection in TNF$^{-/-}$ mice was not associated with the marked pulmonary neutrophil infiltrate and progressive fatal necrosis observed with *M. tuberculosis* infection (Fig. 8) (8, 10). This allowed the identification of three phases in the cellular control of the infection. First, the rapid clearance of *M. smegmatis* during the first week of the infection occurs independently of TNF

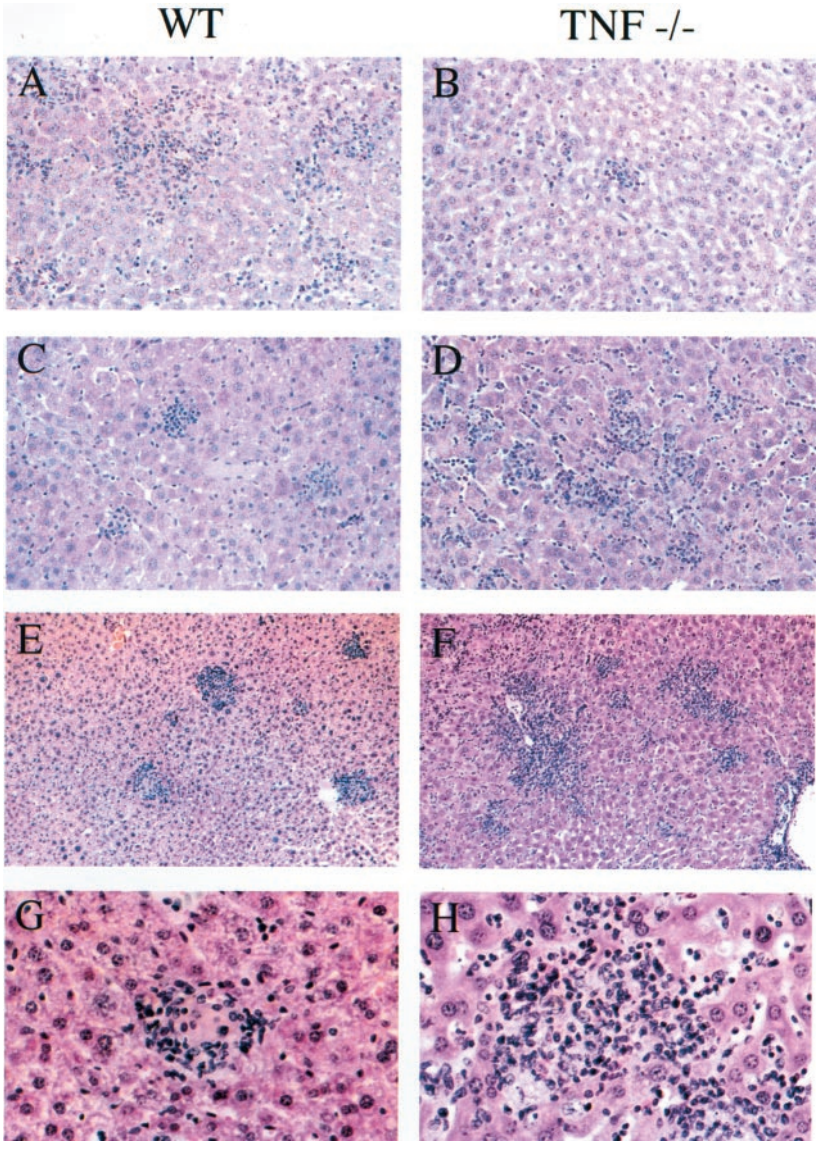

FIGURE 4. Cell recruitment and formation of clusters of leukocytes are delayed in the livers of TNF$^{-/-}$ mice following infection with *M. smegmatis* or *M. tuberculosis* compared with WT mice. *A*, *C*, *E*, and *G*, Representative sections from WT mice; *B*, *D*, *F*, and *H*, representative sections from TNF$^{-/-}$ mice, infected with either *M. smegmatis* (*A–D*) or *M. tuberculosis* (*E–H*). *A* and *B*, Fourteen days postinfection; *C–H*, day 28 postinfection. On day 14 the livers of WT mice infected with *M. smegmatis* were infiltrated with macrophages and lymphocytes (*A*), while in TNF$^{-/-}$ mice the hepatic infiltrate was markedly reduced (*B*). On day 28 of *M. smegmatis* infection, WT mice showed partial resolution of the cellular infiltrate, which formed tight clusters (*C*), while in TNF$^{-/-}$ mice there was a loose infiltrate of lymphocytes and macrophages (*D*). By 28 days of *M. tuberculosis* infection, the leukocyte infiltrate formed tight granulomas in the livers of WT mice (*E*), with lymphocytes surrounding epithelioid macrophages (*G*). In TNF$^{-/-}$ mice infected with *M. tuberculosis*, the diffuse infiltrate failed to form tight granulomas (*F* and *H*). Tissues were sectioned and stained with H&E (original magnification, *A–F*, ×200; *G* and *H*, ×400).

(Fig. 2). Therefore, although the araLAM-rich *M. smegmatis* is a more potent stimulant of TNF production than slow-growing *M. bovis* (BCG) in vitro (Fig. 1), TNF is not required for the initial killing of the organisms in liver and spleen, the major sites of infection. The next phase during wk 2 is characterized in normal mice by a marked influx of macrophages and lymphocytes into the liver that peak on day 14 (Fig. 3) and a progressive decline in bacterial load. This is associated with the induction of both C-C and C-X-C chemokines (Figs. 5 and 6). This phase is dependent on TNF, and in its absence the cellular infiltrate is delayed by 2 wk (Fig. 3). This results in a significant reduction in the rate of clearance of the mycobacteria (Fig. 2). During the third phase in wk 3 and 4, normal mice show progressive clearance of the organisms, with a fall in chemokine mRNA levels and a reduction in the cellular infiltrate. The TNF$^{-/-}$ mice, however, demonstrated further differences during this phase. Transcripts for MIP-2, MCP-1, and MIP-1α appeared by day 21 and had significantly increased by day 28. This was associated with the recruitment of both macrophages and T cells (Fig. 3, *C* and *D*, and Fig. 4) and reduction in the bacterial loads to the levels in WT mice (Fig. 2). In addition, the TNF$^{-/-}$ mice showed significantly greater mycobacteria-specific Th1-like T cell responses by day 28 (Fig. 7), with the concurrent rise of serum nitrate as evidence of the late activation of iNOS (Table I).

These results highlight different aspects of TNF's role in the in vivo control of mycobacterial infection. First, TNF is essential for the early induction of chemokines and subsequent leukocyte recruitment to infected organs, particularly macrophages, which, following activation, produce RNI essential for the clearance of infection in mice. Infection of macrophages with *M. tuberculosis* in vitro leads to the rapid secretion of MIP-1α, MIP-2, and MCP-1 within 12 h (21). However, during low dose aerosol infection with *M. tuberculosis*, transcripts for these chemokines only appeared in the lungs after day 30 (21). By contrast there were small, but significant, increases in chemokine mRNA on days 7–14 in the livers of WT mice following i.v. infection with *M. tuberculosis*, and these levels peaked on day 21 (Fig. 9). In vitro studies with neutralizing anti-TNF Ab showed that the MIP-1α response to *M. avium* infection (22) and the chemokine response in rat lung injury (23) were also dependent on TNF.

Recently, neutralization of TNF in vivo was found to reduce the rapid response of some, but not all, chemokines in an acute model of pulmonary Th_1-like granulomas generated by the injection of

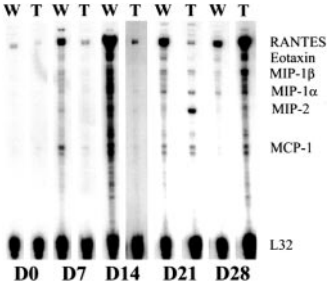

FIGURE 5. Kinetics of chemokine induction following *M. smegmatis* infection in WT and TNF$^{-/-}$ mice. Total liver RNA was isolated and analyzed using a RiboQuant RNase protection assay for the expression of mRNA for lymphotactin, RANTES, eotaxin, MIP-1α, MIP-1β, MIP-2, MCP-1, T cell activation-3, GADPH, and L32. Each lane is representative of one of three mice per group for days 0, 7, 14, 21, and 28 postinfection. (W, WT; T, TNF$^{-/-}$).

purified protein derivative-coated beads (24). Of the 24 chemokines studied, eight, including MIP-2, MIP-1α, and MIP-1β, increased more in PPD-induced than in schistosomal Ag-induced granulomas, with transcript levels peaking at 1–2 days. A further five, including MCP-1, were elevated in both types of granulomas, while eotaxin and three others were elevated in response to schistosomal Ag-induced granulomas. Interestingly, inhibition of TNF reduced by 30–50% the early rise in mRNA for five of the nine chemokines tested, including MIP-1α and MCP-1, but had no effect on the MIP-2 response (24). By contrast, during in vivo infection with *M. smegmatis*, the peak chemokine mRNA in the liver occurred on day 14 (Fig. 5), and only the constitutively expressed RANTES showed a significant rise on day 7 (Fig. 6). Also, there was less apparent selectivity in the pattern of chemokine observed following mycobacterial infection, with induction of eotaxin occurring in both *M. smegmatis*- and *M. tuberculosis*-infected mice (Figs. 6 and 9). Further, all six chemokines examined, including MIP-2, were markedly reduced in TNF-deficient mice, with no response evident on day 14 when the inflammation was peaking in WT mice in response to *M. smegmatis* (Fig. 3). Subsequently, there was delayed induction of chemokine transcription within the liver of TNF$^{-/-}$ mice (Fig. 6), indicating that the chemokine response to persistent infection was not completely dependent on TNF.

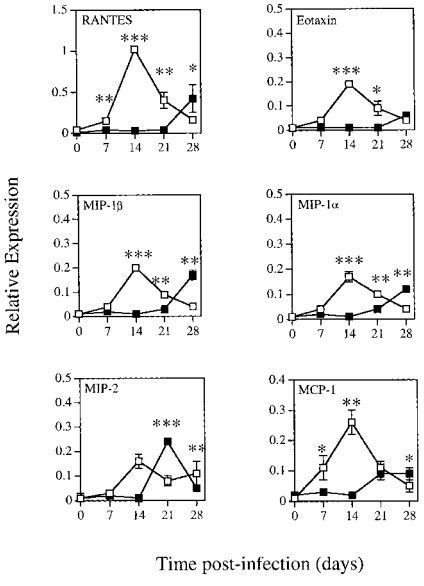

FIGURE 6. Relative expression of chemokine mRNA in the livers of WT (□) and TNF$^{-/-}$ (■) mice following i.v. infection with *M. smegmatis*. Total liver RNA was isolated from mice over the course of the infection and then analyzed by RNase protection assay. The data are expressed as the ratio of chemokine gene expression to a constitutively expressed gene (L32) for RANTES (*A*), eotaxin (*B*), MIP-1β (*C*), MIP-1α (*D*), MIP-2 (*E*), and MCP-1 (*F*). Each data point is the mean ± SEM for three mice, and data are representative of one of two experiments. Significant differences between TNF$^{-/-}$ and WT mice (*, $p < 0.05$; **, $p < 0.01$; and ***, $p < 0.0001$) were determined by Student's *t* test.

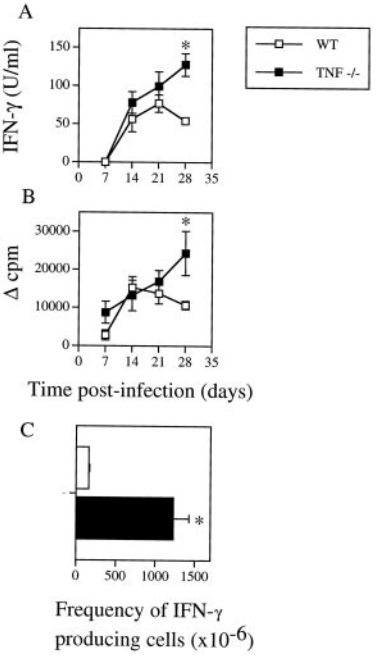

FIGURE 7. Ag-specific T cell responses in WT (□) and TNF$^{-/-}$ (■) mice infected with *M. smegmatis*. *A* and *B*, Splenocytes were cultured in the presence of *M. smegmatis* sonicate (10 μg/ml) for 3 days. IFN-γ production was measured by ELISA (*A*), and proliferation was determined by the incorporation of [^{3}H]thymidine over the final 6 h of culture (*B*). *C*, Splenocytes from day 28 postinfection were cultured in the presence of *M. smegmatis* sonicate (10 μg/ml) overnight, and the frequency of IFN-γ-producing cells was determined by ELISPOT assay. Ag-specific results were obtained by subtracting the mean IFN-γ levels, thymidine incorporation into cells, and frequency of IFN-γ-producing splenocytes cultured without sonicate. The data are the mean ± SEM of five mice per group and are representative of one of two experiments. Significant differences between TNF$^{-/-}$ and WT mice (*, $p < 0.05$) were determined by Student's *t* test.

This TNF-independent component of the chemokine response was more evident during infection with the more virulent *M. tuberculosis*. There were lower chemokine transcript levels in

Table I. *Production of RNI in WT and TNF$^{-/-}$ mice following infection with* M. smegmatis

Time Postinfection (days)	WT[a] (μM)	TNF$^{-/-a}$ (μM)
0	18.3 (1.3)	14.6 (6.4)
7	57.7 (2.5)	36.6 (3.5)
14	239.1 (52.5)	68.3 (31.6)
21	80.4 (14.7)	71.1 (19.4)
28	47.2 (6.2)	212.8 (40)

[a] The mean (±SEM) concentration of total serum nitrites in the sera of four WT and four TNF$^{-/-}$ animals at each time point. This is representative of one of two experiments. Total serum nitrate was reduced by nitrate reductase to nitrite and measured by the Greiss reagent. Significant differences between TNF$^{-/-}$ and WT mice (*, $p < 0.05$; **, $p < 0.02$) were determined using Student's *t* test.

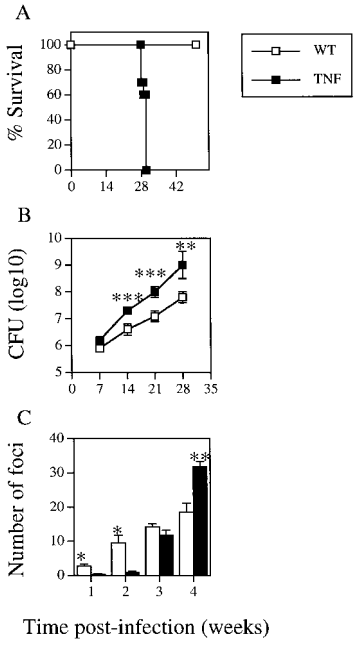

FIGURE 8. TNF$^{-/-}$ mice succumb to i.v. infection with *M. tuberculosis* with delayed formation of liver granulomas. WT (□) and TNF$^{-/-}$ (■) mice were infected with 1×10^4 CFU *M. tuberculosis* H37Rv i.v., and the course of infection was monitored over time. *A*, Survival of mice following infection ($n = 8$). *B*, The numbers of viable bacteria present in liver. The data points are the mean ± SEM of the mycobacterial colony-forming units from four mice per time point. *C*, The numbers of foci of inflammatory cells in the livers of WT and TNF$^{-/-}$ mice. The data points are the mean ± SEM of the number of foci from four mice per time point. Significant differences between TNF$^{-/-}$ and WT mice (*, $p < 0.05$) were determined by Student's *t* test.

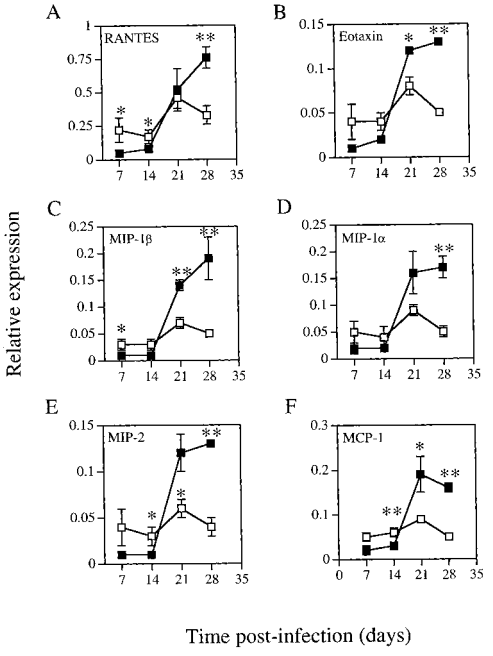

FIGURE 9. Relative expression of chemokine mRNA in the livers of WT (□) and TNF$^{-/-}$ (■) mice following i.v. infection with *M. tuberculosis*. Total liver RNA was isolated then analyzed by RNase protection assay. The data are expressed as the ratio of chemokine gene expression to a constitutively expressed gene (L32) for RANTES (*A*), eotaxin (*B*), MIP-1β (*C*), MIP-1α (*D*), MIP-2 (*E*), and MCP-1 (*F*). Each data point is the mean ± SEM for three mice. Significant differences between TNF$^{-/-}$ and WT mice (*, $p < 0.05$; **, $p < 0.01$) were determined by Student's *t* test.

TNF$^{-/-}$ mice compared with WT mice early in *M. tuberculosis* infection, but by day 21 there were significant increases in hepatic mRNA for both the C-C and C-X-C chemokines, to levels higher than those in WT mice (Fig. 8). These continued to rise during the last week of the fatal infection. *M. bovis* (BCG) infection of TNF-deficient mice was also associated with comparable increases in chemokine mRNA expression (25) and in MCP-1 and MIP-1α protein levels compared with WT mice (26). Furthermore, delayed expression of MIP-1α and MIP-1β mRNA was observed in TNF/LT$\alpha^{-/-}$ double-knockout mice (25). This late excessive chemokine response to *M. tuberculosis* or *M. bovis* in TNF$^{-/-}$ mice was associated with a delayed or aberrant inflammatory response with failure to control the infection (10, 25, 26). Therefore, in addition to its role in the initial cellular recruitment, TNF plays an essential role in regulation of the inflammatory response and, in particular, the juxtaposition of macrophages and lymphocytes to form granulomas. This was evident in both *M. smegmatis* and *M. tuberculosis* infection, where, despite the influx of leukocytes, there is failure to form the tight foci of leukocytes evident in the liver of WT mice (Fig. 4). The inadequate migration of lymphocytes into *M. tuberculosis* infection in TNF deficiency may relate to the binding of TNF to the extracellular matrix to direct migration leukocytes through tissues (27). TNF may also contribute to the tight apposition of macrophages and lymphocytes within granulomas, either as secreted or membrane-bound forms. TNF is highly expressed within granulomas in human tuberculosis (28), leprosy (29), and murine (7) mycobacterial infections and is essential for the differentiation of macrophages into epithelioid cells. Neutralization of TNF activity in established mycobacterial infections leads to the disruption of granulomas, with recrudescence and dissemination of the *M. tuberculosis* infection (30–32).

A further effect of TNF deficiency on *M. smegmatis* infection was the enhanced T cell response later in the infection (Fig. 7). Previously, normal T cell responses have been demonstrated in TNF$^{-/-}$ mice to keyhole limpet hemocyanin and alloantigens (38), mycobacterial Ags (8, 10), and autoantigens (33). The enhanced T cell response during *M. smegmatis* infection (Fig. 7) was probably due to the increased bacterial load seen in TNF$^{-/-}$ from wk 2 to 3 of infection (Fig. 2). Previously, we have expressed *M. tuberculosis* genes in *M. smegmatis* (34), but found the recombinant *M. smegmatis* relatively poor at inducing T cell responses to the exogenous Ag in comparison to recombinant *M. bovis* (BCG) (18) (P. W. Roche, unpublished observations), presumably due to the rapid clearance of *M. smegmatis* in normal mice. In the absence of TNF, the enhanced T cell response with increased IFN-γ production on day 28 may have contributed to the eventual clearance of the organisms. T cells are a potent source of LTα (35) that may also activate macrophages through TNF receptor I, resulting in iNOS induction (36) and increased killing of the bacterium. Recent studies with LT$\alpha^{-/-}$ chimeras (11) or LTα/TNF$^{-/-}$ mice reconstituted with TNF-α transgenes (25) have confirmed that LTα is essential to control *M. tuberculosis* and BCG infection as well as infection with *L. monocytogenes* infection (D. R. Roach, unpublished observation). Nevertheless, LTα is unable to complement for the effects of TNF deficiency in TNF$^{-/-}$ mice infected with *M. tuberculosis*.

In summary, TNF was essential for the early induction of chemokines and leukocyte recruitment following *M. smegmatis* infection in the liver, but this defect was compensated by a later chemokine response with enhanced Th1-like T cell response that

controlled the infection. With the more virulent *M. tuberculosis* infection, after an initial delay in chemokine response there was a marked TNF-independent rise in chemokines, but the inflammatory response was dysregulated, with failure to form effective tight granulomas. The importance of TNF-dependent granuloma formation in the control of latent *M. tuberculosis* infection in humans is graphically illustrated by the rapid reactivation of clinical tuberculosis in patients undergoing treatment for rheumatoid arthritis and Crohn's disease with a humanized mAb to TNF (37).

Acknowledgments

We thank A. Spinoulas and J. Compton for their technical assistance, and Drs. J. Sedgwick and B. Saunders for their helpful discussion.

References

1. Flynn, J. L., and J. Chan. 2001. Immunology of tuberculosis. *Annu. Rev. Immunol. 19:93.*
2. Cooper, A. M., D. K. Dalton, T. A. Stewart, J. P. Griffin, D. G. Russell, and I. M. Orme. 1993. Disseminated tuberculosis in interferon γ gene-disrupted mice. *J. Exp. Med. 178:2243.*
3. Feng, C. G., A. G. D. Bean, H. Hooi, H. Briscoe, and W. J. Britton. 1999. Increase in γ interferon-secreting $CD8^+$, as well as $CD4^+$, T cells in lungs following aerosol infection with *Mycobacterium tuberculosis*. *Infect. Immun. 67: 3242.*
4. Feng, C. G., W. J. Britton, U. Palendira, N. L. Groat, H. Briscoe, and A. G. Bean. 2000. Up-regulation of VCAM-1 and differential expansion of β integrin-expressing T lymphocytes are associated with immunity to pulmonary *Mycobacterium tuberculosis* infection. *J. Immunol. 164:4853.*
5. Orme, I. M., and F. M. Collins. 1994. Mouse model of tuberculosis. In *Tuberculosis: Pathogenesis, Protection and Control*. B. B. Bloom, ed. American Society for Microbiology, Washington, DC, p. 113.
6. Orme, I. M. 1998. The immunopathogenesis of tuberculosis: a new working hypothesis. *Trends Microbiol. 6:94.*
7. Kindler, V., A. P. Sappino, G. E. Grau, P. F. Piguet, and P. Vassalli. 1989. The inducing role of tumor necrosis factor in the development of bactericidal granulomas during BCG infection. *Cell 56:731.*
8. Flynn, J. L., M. M. Goldstein, J. Chan, K. J. Triebold, K. Pfeffer, C. J. Lowenstein, R. Schreiber, T. W. Mak, and B. R. Bloom. 1995. Tumor necrosis factor-α is required in the protective immune response against *Mycobacterium tuberculosis* in mice. *Immunology 2:561.*
9. Sedgwick, J. D., D. S. Riminton, J. G. Cyster, and H. Korner. 2000. Tumor necrosis factor: a master-regulator of leukocyte movement. *Immunol. Today 21: 110.*
10. Bean, A. G. D., D. R. Roach, H. Briscoe, M. P. France, H. Korner, J. D. Sedgwick, and W. J. Britton. 1999. Structural deficiencies in granuloma formation in TNF gene-targeted mice underlie the heightened susceptibility to aerosol *Mycobacterium tuberculosis* infection, which is not compensated for by lymphotoxin. *J. Immunol. 162:3504.*
11. Roach, D. R., H. Briscoe, B. Saunders, M. P. France, S. Riminton, and W. J. Britton. 2001. Secreted lymphotoxin-α is essential for the control of an intracellular bacterial infection. *J. Exp. Med. 193:239.*
12. Hunter, S. W., H. Gaylord, and P. J. Brennan. 1986. Structure and antigenicity of the phosphorylated lipopolysaccharide antigens from the leprosy and tubercle bacilli. *J. Biol. Chem. 261:12345.*
13. Chatterjee, D., C. M. Bozic, M. McNeil, and P. J. Brennan. 1991. Structural features of the arabinan component of the lipoarabinomannan of *Mycobacterium tuberculosis*. *J. Biol. Chem. 266:9652.*
14. Chatterjee, D., K. H. Khoo, M. R. McNeil, A. Dell, H. R. Morris, and P. J. Brennan. 1993. Structural definition of the non-reducing termini of mannose-capped LAM from *Mycobacterium tuberculosis* through selective enzymatic degradation and fast atom bombardment-mass spectrometry. *Glycobiology 3:497.*
15. Chatterjee, D., A. D. Roberts, K. Lowell, P. J. Brennan, and I. M. Orme. 1992. Structural basis of capacity of lipoarabinomannan to induce secretion of tumor necrosis factor. *Infect. Immun. 60:1249.*
16. Roach, T. I., C. H. Barton, D. Chatterjee, and J. M. Blackwell. 1993. Macrophage activation: lipoarabinomannan from avirulent and virulent strains of *Mycobacterium tuberculosis* differentially induces the early genes c-*fos*, KC, JE, and tumor necrosis factor-α. *J. Immunol. 150:1886.*
17. Korner, H., M. Cook, D. S. Riminton, F. A. Lemckert, R. M. Hoek, B. Ledermann, F. Kontgen, B. F. Destgroth, and J. D. Sedgwick. 1997. Distinct roles for lymphotoxin-α and tumour necrosis factor in organogenesis and spatial organization of lymphoid tissue. *Eur. J. Immunol. 27:2600.*
18. Martin, E., A. T. Kamath, J. A. Triccas, and W. J. Britton. 2000. Protection against virulent *Mycobacterium avium* infection following DNA vaccination with the 35-kilodalton antigen is accompanied by induction of γ interferon-secreting $CD4^+$ T cells. *Infect. Immun. 68:3090.*
19. Kamath, A. T., C. G. Feng, M. Macdonald, H. Briscoe, and W. J. Britton. 1999. Differential protective efficacy of DNA vaccines expressing secreted proteins of *Mycobacterium tuberculosis*. *Infect. Immun. 67:1702.*
20. Barry, C. E. 2001. *Mycobacterium smegmatis*: an absurd model for tuberculosis? *Trends Microbiol. 9:473.*
21. Rhoades, E. R., A. M. Cooper, and I. M. Orme. 1995. Chemokine response in mice infected with *Mycobacterium tuberculosis*. *Infect. Immun. 63:3871.*
22. Smith, D., H. Hansch, G. Bancroft, and S. Ehlers. 1997. T-cell-independent granuloma formation in response to *Mycobacterium avium*: role of tumour necrosis factor-α and interferon-γ. *Immunology 92:413.*
23. Czermak, B. J., V. Sarma, N. M. Bless, H. Schmal, H. P. Friedl, and P. A. Ward. 1999. In vitro and in vivo dependency of chemokine generation on C5a and TNF-α. *J. Immunol. 162:2321.*
24. Qiu, B., K. A. Frait, F. Reich, E. Komuniecki, and S. W. Chensue. 2001. Chemokine expression dynamics in mycobacterial (type-1) and schistosomal (type-2) antigen-elicited pulmonary granuloma formation. *Am. J. Pathol. 158:1503.*
25. Bopst, M., I. Garcia, R. Guler, M. L. Olleros, T. Rulicke, M. Muller, S. Wyss, K. Frei, M. Le Hir, and H. P. Eugster. 2001. Differential effects of TNF and LTα in the host defense against *M. bovis* BCG. *Eur. J. Immunol. 31:1935.*
26. Jacobs, M., M. W. Marino, N. Brown, B. Abel, L. G. Bekker, V. J. F. Quesniaux, L. Fick, and B. Ryffel. 2000. Correction of defective host response to *Mycobacterium bovis* BCG infection in TNF-deficient mice by bone marrow transplantation. *Lab. Invest. 80:901.*
27. Franitza, S., R. Hershkoviz, N. Kam, N. Lichtenstein, G. G. Vaday, R. Alon, and O. Lider. 2000. TNF-α associated with extracellular matrix fibronectin provides a stop signal for chemotactically migrating T cells. *J. Immunol. 165:2738.*
28. Barnes, P. F., S. J. Fong, P. J. Brennan, P. E. Twomey, A. Mazumder, and R. L. Modlin. 1990. Local production of tumor necrosis factor and IFN-γ in tuberculous pleuritis. *J. Immunol. 145:149.*
29. Khanolkaryoung, S., N. Rayment, P. M. Brickell, D. R. Katz, S. Vinayakumar, M. J. Colston, and D. N. J. Lockwood. 1995. Tumour necrosis factor-α (TNF-α) synthesis is associated with the skin and peripheral nerve pathology of leprosy reversal reactions. *Clin. Exp. Immunol. 99:196.*
30. Flynn, J. L., and J. Chan. 2001. Tuberculosis: latency and reactivation. *Infect. Immun. 69:4195.*
31. Turner, J., A. A. Frank, J. V. Brooks, P. M. Marietta, and I. M. Orme. 2001. Pentoxifylline treatment of mice with chronic pulmonary tuberculosis accelerates the development of destructive pathology. *Immunology 102:248.*
32. Mohan, V. P., C. A. Scanga, K. Yu, H. M. Scott, K. E. Tanaka, E. Tsang, M. C. Tsai, J. L. Flynn, and J. Chan. 2001. Effects of tumor necrosis factor α on host immune response in chronic persistent tuberculosis: possible role for limiting pathology. *Infect. Immun. 69:1847.*
33. Korner, H., D. S. Riminton, D. H. Strickland, F. A. Lemckert, J. D. Pollard, and J. D. Sedgwick. 1997. Critical points of tumor necrosis factor action in central nervous system autoimmune inflammation defined by gene targeting. *J. Exp. Med. 186:1585.*
34. Roche, P. W., N. Winter, J. A. Triccas, C. G. Feng, and W. J. Britton. 1996. Expression of *Mycobacterium tuberculosis* MPT64 in recombinant *Myco. smegmatis*: purification, immunogenicity and application to skin tests for tuberculosis. *Clin. Exp. Immunol. 103:226.*
35. Ohshima, Y., L. P. Yang, M. N. Avice, M. Kurimoto, T. Nakajima, M. Sergerie, C. E. Demeure, M. Sarfati, and G. Delespesse. 1999. Naive human $CD4^+$ T cells are a major source of lymphotoxin α. *J. Immunol. 162:3790.*
36. Matsushima, H., M. Shirai, K. Ouchi, K. Yamashita, T. Kakutani, S. Furukawa, and T. Nakazawa. 1999. Lymphotoxin inhibits *Chlamydia pneumoniae* growth in HEp-2 cells. *Infect. Immun. 67:3175.*
37. Keane, J., S. Gershon, R. P. Wise, E. Mirabile-Levens, J. Kasznica, W. D. Schwieterman, J. N. Siegel, and M. M. Braun. 2001. Tuberculosis associated with infliximab, a tumor necrosis factor α-neutralizing agent. *N. Engl. J. Med. 345:1098.*
38. Marino, M. W., A. Dunn, D. Grail, M. Inglese, Y. Noguchi, E. Richards, A. Jungbluth, H. Wada, M. Moore, B. Williamson, et al. 1997 Characterization of tumor necrosis factor-deficient mice. *Proc. Natl. Acad. Sci. USA 94:8093.*